Discrete-to-Continuum Metrics from Scalar Fields

LARS RÖNNBÄCK
Stockholm University
lars@uptochange.com

Abstract

We present seam-driven geometry*, a scalar-first framework for geometry processing in which geometric structure is generated from a scalar field $s : U \to \mathbb{R}$ (a* seam*) via an explicit local* Rule $\mathcal{R}$*. In the discrete setting, we study a conformal graph rule that assigns edge lengths using an endpoint quadrature of e^s, yielding a shortest-path metric that is easy to optimize and differentiate. Our main results are (i) a quantitative discrete-to-continuum guarantee for seam-generated shortest-path metrics on graph families whose shortest-path distances approximate background geodesic distance up to an additive $O(h)$ error (e.g., sufficiently dense neighborhood graphs); (ii) a curvature sensitivity identity showing that first-order curvature variations are governed by the cotangent Laplacian; and (iii) a strictly convex inverse-design formulation for fitting target edge weights via a quadratic program in variables $X_u = e^{s(u)}$. These results position seams as a stable interface between differential-geometric objectives and practical optimization pipelines in mesh and graph processing.*

Keywords: seam-driven geometry; discrete conformal metric; Gromov–Hausdorff convergence; signless Laplacian; inverse metric design.

1 Introduction

Standard presentations of geometry begin with a metric or a manifold structure postulated *a priori*. Here we emphasize a complementary, constructive viewpoint: start with a base space U and a scalar field s (the *seam*), then let an explicit Rule $\mathcal{R}$ produce the geometric data.

In smooth differential geometry, this scalar-first perspective provides an elegant synthesis. Conformal metrics, Information Geometry (Hessian metrics), optimal transport (Kantorovich potentials), and Morse handle-bodies can all be viewed as the output of specific local operations on a scalar field. However, the true utility of this formulation arises in computational and applied mathematics. On discrete meshes, manipulating full tensor fields is algorithmically cumbersome and numerically unstable. By reducing metric generation to the evaluation of a scalar seam, highly complex geometric problems (like metric projection or feature-aware routing) can be reduced to fast, stable scalar optimization.

In this paper, we formally define the Seam-Rule framework and demonstrate its utility. Section 2 establishes the formal axioms and composition laws for Rules, and Section 3 catalogs standard

continuous and discrete Rules. This axiomatic layer is intended primarily as a unifying *language* for organizing constructions across settings (and can be skimmed on a first, results-focused read). Section 4 illustrates how familiar continuous identities (e.g., Gauss–Bonnet) are cleanly expressed in the seam-rule viewpoint. Finally, Section 5 provides the computational core: proving that seam-generated shortest-path metrics on suitable graph families approximate smooth conformal metrics, identifying a cotangent-Laplacian curvature sensitivity, and enabling strictly convex inverse metric design.

Contributions (geometry processing view). Our contributions are geared toward mesh and graph processing, where one seeks parameterizations that are easy to optimize, differentiate, and analyze.

1. **A scalar-first metric parameterization on graphs/meshes.** We study a conformal graph rule that assigns edge lengths using an endpoint quadrature of e^s, producing a shortest-path metric with local control by a scalar seam.
2. **Quantitative discrete-to-continuum guarantees.** Under an asymptotically geodesic spanner hypothesis for the background shortest-path metric (as is standard for sufficiently dense neighborhood graphs), we prove an $O(h)$ Gromov–Hausdorff convergence rate between the seam-generated discrete metric and the smooth conformal metric (Theorem 3) and derive a corresponding uniform $O(h)$ metric error bound (Theorem 4).
3. **Curvature sensitivity via cotangent weights.** We show that the *first-order* (Jacobian) sensitivity of angle-defect curvature with respect to the seam exactly matches the cotangent Laplacian (with the standard scaling used in discrete differential geometry) at $s = 0$ (Theorem 7), providing a differentiable link between scalar parameters and discrete curvature.
4. **Convex inverse metric design.** We reduce edge-weight fitting under the conformal graph rule to a strictly convex quadratic program in variables $X_u = e^{s(u)}$ on non-bipartite graphs (Theorem 5), leveraging a classical signless-Laplacian positive-definiteness criterion [9, 10]. We further provide gauge-fixing and conditioning guarantees (Theorem 6).

1.1 Related Work

Scalar fields on meshes are a classical and widely used representation in geometry processing, in particular as vertex-based conformal factors and potentials. Discrete uniformization and discrete conformal parameterizations seek a scalar conformal scaling that induces a metric of prescribed curvature or that supports flattening/parameterization; see, e.g., Gu–Luo–Sun–Wu [12] and the variational formulations of Springborn–Schröder–Pinkall [13]. In this literature, a scalar field (often a log-scale factor) is the primary unknown, and the induced metric is obtained by a local rule that rescales discrete lengths/angles.

Circle packing provides another scalar-first route to discrete conformal geometry, in which circle radii (or log-radii) act as scalar variables whose induced intersection patterns and edge lengths encode a discrete conformal structure; see Stephenson [17] for an overview and references. Closely related, combinatorial Ricci flow evolves a vertex-based scalar parameterization (e.g., circle radii or log-scale factors) to drive discrete curvature toward a target, with Chow–Luo [16] as a foundational reference.

More broadly, discrete-to-continuum limits are a recurring theme in discrete differential geometry: as triangulations refine, one seeks conditions under which discrete conformal structures and

their induced metrics converge (in appropriate senses) to their smooth counterparts; see, e.g., the discrete conformal/uniformization viewpoints in [11, 12] and references therein.

Our intent is not to claim novelty of using scalar fields per se, but to formalize a general "seam $\to$ rule $\to$ geometry" interface that accommodates multiple continuous and discrete constructions under one axiomatic umbrella, and to highlight algorithmic consequences of a particular discrete edge-length rule: a quantitative discrete-to-continuum guarantee for the resulting shortest-path metric, a curvature sensitivity identity, and a convex inverse-design formulation for fitting target edge weights.

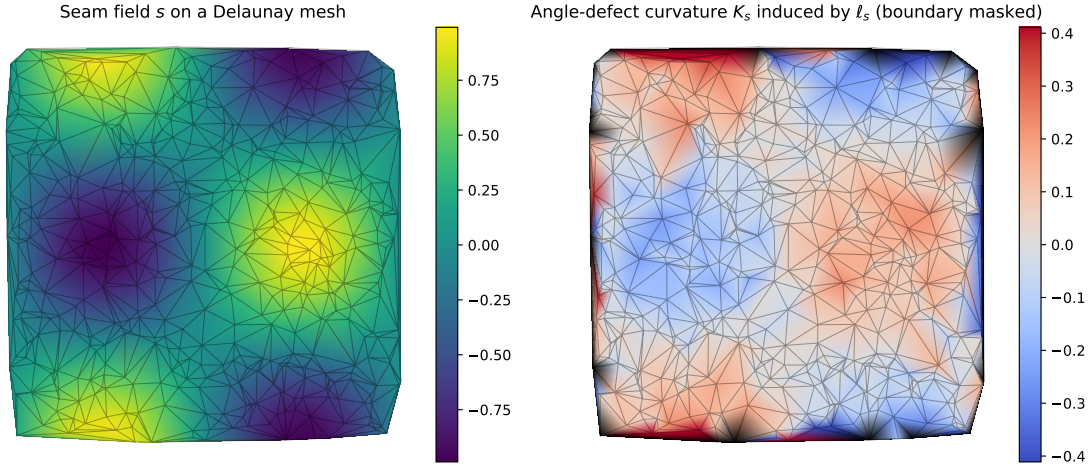

Figure 1: A small Delaunay mesh colored by the seam field s (left) and the induced discrete Gaussian curvature K_s (angle defect) computed from the seam-generated intrinsic edge lengths $\ell_s(u,v) = \ell_0(u,v)\frac{e^{s(u)}+e^{s(v)}}{2}$ (right; boundary vertices masked to avoid boundary angle-defect dominance).

2 Framework: Seams, Rules, and Composition

Let U be a paracompact Hausdorff space (or discrete set) equipped with a local background structure $\mathcal{T}_U$ (e.g., a differentiable atlas, a background metric h, or a graph adjacency).

Definition 1. *A* seam *is a function $s : U \to \mathbb{R}$ belonging to an admissible class $\mathcal{S}(U)$ (e.g., C^∞, Morse, convex, or discrete array). The seam acts as the generative potential for local geometry.*

Definition 2. *A* Rule *is a natural, local assignment $\mathcal{R}$ that takes admissible seam data $(U, s, \mathcal{T}_U)$ to a geometric output G (e.g., a pseudo-metric D, tensor g, or weighted graph). A valid Rule must satisfy:*

1. ***Locality:*** *For every open $V \subseteq U$, the output on V depends only on $s|_V$ and $\mathcal{T}_U|_V$.*
2. ***Gluing (Sheaf Condition):*** *If $\{V_\alpha\}$ covers U and the locally generated outputs $G_\alpha = \mathcal{R}(V_\alpha, s|_{V_\alpha})$ agree on overlaps, there is a unique global object G such that $G|_{V_\alpha} = G_\alpha$.*

3. ***Functoriality:*** *For every structure-preserving map $\varphi : U \to U'$, one has $\mathcal{R}(U, \varphi^* s') = \varphi^* \mathcal{R}(U', s')$.*

Remark 1 (Scope of the axioms). The Functoriality axiom is to be interpreted relative to the chosen background structure: in the smooth setting, φ is typically a smooth map compatible with the chosen atlas/connection (or a diffeomorphism when tensors are pulled back); in the discrete setting, φ is typically a graph isomorphism or a map preserving adjacency/weights. Likewise, the Gluing axiom is automatic for sheaf-like outputs (e.g., smooth tensor fields), while for global outputs (e.g., a distance function on all of $U \times U$) the condition should be read as compatibility of the induced restrictions on each $V_\alpha \times V_\alpha$.

If the generated output is a distance function D, it must satisfy the standard pseudo-metric axioms (non-negativity, identity, symmetry, and triangle inequality).

A powerful feature of this axiomatic formulation is that it allows for the rigorous chaining of Rules, enabling complex geometries to be built from multiple scalar layers.

Proposition 1. *Let $\mathcal{R}_1$ and $\mathcal{R}_2$ be Rules in the sense of Definition 2. Suppose $\mathcal{R}_1$ maps $(U, s_1, \mathcal{T}_U)$ to an intermediate background structure $\mathcal{T}'_U := \mathcal{R}_1(U, s_1)$, and $\mathcal{R}_2$ maps $(U, s_2, \mathcal{T}'_U)$ to a geometric output $G := \mathcal{R}_2(U, s_2; \mathcal{T}'_U)$. Then the composed assignment*

$$\mathcal{R}_{2\circ 1}(U, (s_1, s_2)) \;:=\; \mathcal{R}_2\big(U, s_2;\, \mathcal{R}_1(U, s_1)\big)$$

is again a Rule (it satisfies Locality, Gluing, and Functoriality).

Proof. Locality follows immediately from the locality of $\mathcal{R}_1$ and $\mathcal{R}_2$: restricting to $V \subseteq U$ yields

$$\mathcal{R}_{2\circ 1}\big(V, (s_1|_V, s_2|_V)\big) = \mathcal{R}_2\big(V, s_2|_V;\, \mathcal{R}_1(V, s_1|_V)\big) = \big(\mathcal{R}_2(U, s_2; \mathcal{R}_1(U, s_1))\big)\big|_V.$$

Gluing holds because $\mathcal{R}_1$ glues local outputs into a unique global $\mathcal{T}'_U$, and then $\mathcal{R}_2$ glues local outputs (using that same $\mathcal{T}'_U$ as background) into a unique global G.

For functoriality, let $\varphi : U \to U'$ be a structure-preserving map and let s'_1, s'_2 be seams on U'. Write $\mathcal{T}'_{U'} := \mathcal{R}_1(U', s'_1)$. Using functoriality of $\mathcal{R}_1$ (since it is a Rule), we have

$$\varphi^* \mathcal{T}'_{U'} = \varphi^* \mathcal{R}_1(U', s'_1) = \mathcal{R}_1(U, \varphi^* s'_1).$$

Now apply functoriality of $\mathcal{R}_2$ (again since it is a Rule), treating the intermediate background as part of its admissible input data:

$$\varphi^* \mathcal{R}_{2\circ 1}(U', (s'_1, s'_2)) = \varphi^* \mathcal{R}_2(U', s'_2; \mathcal{T}'_{U'}) = \mathcal{R}_2(U, \varphi^* s'_2; \varphi^* \mathcal{T}'_{U'}) = \mathcal{R}_2(U, \varphi^* s'_2; \mathcal{R}_1(U, \varphi^* s'_1)) = \mathcal{R}_{2\circ 1}(U, (\varphi^* s'_1, \varphi^* s'_2)).$$

This is exactly the Functoriality axiom for the composed Rule. □

3 The Repertoire of Rules

The generative power of the framework relies on specific definitions of $\mathcal{R}$.

3.1 Continuous Rules

For a smooth manifold U, we highlight three primary rules generating metric tensors g:

1. **The Hessian Rule ($\mathcal{R}_{\text{Hessian}}$):** $g = \nabla^2 s$ for a chosen torsion-free connection ∇ (in local affine coordinates: $g_{ij} = \partial_i \partial_j s$). Where g is positive definite (e.g., for strictly convex s), it defines a Riemannian metric locally (as proven later in Theorem 2). In general, $\nabla^2 s$ may be indefinite; allowing such outputs naturally leads to pseudo-Riemannian geometries, which we do not develop here. Hessian geometry is central to Information Geometry [1, 2].
2. **The Conformal Rule ($\mathcal{R}_{\text{Conf}}$):** $g_{ij} = e^{2s} h_{ij}$. Generates geometries conformally equivalent to a background metric h [3].
3. **The Gradient Rule ($\mathcal{R}_{\text{Grad}}$):** $g_{ij} = |\nabla s|_h^2 h_{ij}$. A subset of conformal geometries controlled by the eikonal magnitude of the seam [4].

Remark 2 (A degenerate table entry). In Table 1, the Flat Torus row is intentionally simple: for the linear seam $s = x^1$ on a flat background one has $|\nabla s|_h \equiv 1$, so the gradient rule yields $g = |\nabla s|_h^2 \, h = h$. Nontrivial behavior under $\mathcal{R}_{\text{Grad}}$ requires a seam with nonconstant gradient magnitude (and, if one wants a genuine Riemannian metric everywhere, bounded away from zero).

Remark 3 (Pseudo-Riemannian outputs are out of scope). The Minkowski example in Table 1 is included only as an illustrative reminder that seam rules can generate familiar tensors: for $s = \frac{1}{2}(t^2 - x^2 - y^2 - z^2)$ one has $\nabla^2 s = \text{diag}(1, -1, -1, -1)$, which is *not* positive definite. The present paper focuses on (local) Riemannian metrics produced where the generated tensor is positive definite; extending the framework systematically to pseudo-Riemannian metrics is an interesting direction but is not pursued here.

Remark: The framework easily recovers classical topological and relativistic results. For instance, applying a piecewise local $\mathcal{R}_{\text{Hessian}}$ stitched by $\mathcal{R}_{\text{Conf}}$ to a Morse seam with two critical points reconstructs Reeb's Sphere Theorem [5]. Similarly, applying a generalized Warped-Product rule to a generic radial seam recovers Birkhoff's Theorem for spherically symmetric vacuum solutions [6].

3.2 Discrete Rules ($\mathcal{R}_{\text{Graph}}$)

On a graph $G = (V, E)$ with background edge lengths $\ell_0(u, v)$, the seam $s : V \to \mathbb{R}$ generates a discrete shortest-path metric D via edge weights $w(u, v)$. Two vital implementations are:

1. **Conformal Graph Rule ($\mathcal{R}_{\text{Graph-Exp}\ s}$):** $w(u, v) = \ell_0(u, v) \frac{e^{s(u)} + e^{s(v)}}{2}$

Table 1: Classical Geometries as Seam-Rule Triplets

Geometry	**Rule**	**Background**	**Seam** s
Euclidean $\mathbb{E}^n$	$\mathcal{R}_{\text{Hessian}}$	None	$\frac{1}{2}\sum (x^i)^2$
Minkowski $\mathbb{M}^4$ (Lorentzian)	$\mathcal{R}_{\text{Hessian}}$	None	$\frac{1}{2}(t^2 - x^2 - y^2 - z^2)$
Poincaré Half-Plane	$\mathcal{R}_{\text{Conf}}$	Euclidean δ_{ij}	$\ln(R) - \ln(y)$
Stereographic Sphere	$\mathcal{R}_{\text{Conf}}$	Euclidean δ_{ij}	$\ln(2R^2) - \ln(R^2 + r^2)$
Flat Torus $\mathbb{T}^2$	$\mathcal{R}_{\text{Grad}}$	Euclidean δ_{ij}	x^1 (linear)

2. **Gradient Graph Rule ($\mathcal{R}_{\text{Graph-}|\nabla s|}$):** $w(u,v) = \ell_0(u,v)\frac{|\nabla s|(u)+|\nabla s|(v)}{2}$

Remark 4 (Arithmetic mean vs. the classical geometric mean). In much of the discrete conformal literature on triangle meshes, a common vertex-based conformal scaling takes the *geometric mean* of endpoint factors, i.e.

$$\ell_s^{\text{geom}}(u,v) = \ell_0(u,v)\,\exp\Big(\tfrac{1}{2}\big(s(u)+s(v)\big)\Big) = \ell_0(u,v)\,\sqrt{e^{s(u)}e^{s(v)}}.$$

By contrast, our Conformal Graph Rule uses the *arithmetic mean*

$$\ell_s^{\text{arith}}(u,v) = \ell_0(u,v)\,\tfrac{1}{2}\big(e^{s(u)}+e^{s(v)}\big).$$

We deviate from the geometric-mean convention intentionally. The arithmetic mean is exactly the endpoint trapezoidal quadrature for the conformal line element $\int e^s \, \mathrm{d}\ell_0$ (Lemma 2), and it is the choice that makes inverse edge-weight fitting *quadratic* in the variables $X_u := e^{s(u)}$ (Theorem 5), yielding a strictly convex QP on non-bipartite graphs. In other words, the arithmetic rule is selected for its discrete-to-continuum consistency and its algorithmic convexity properties, not because it is the only possible discrete conformal scaling.

These constructions are closely related to discrete conformal geometry and conformal parameterizations of triangle meshes; see, e.g., [13, 12]. They also connect to circle-packing/combinatorial Ricci flow viewpoints on discrete conformal scaling [16] and to related conformal-type transformations such as spin transformations [14].

4 Continuous Geometry: Curvature Identities

Framing continuous geometry in terms of seams often reduces complex tensor algebra to elegant scalar identities.

Theorem 1 (Gauss–Bonnet via a seam)**.** *Let (M,g) be a closed oriented Riemannian surface. By the uniformization theorem, there exists a metric h of constant Gaussian curvature and a seam s such that $g = \mathcal{R}_{Conf}(s;h) = e^{2s}h$. Then $\int_M K_g \, dA_g = 2\pi\chi(M)$.*

Proof. Under the conformal rule, curvature transforms as $K_g = e^{-2s}(K_h - \Delta_h s)$, and the area form as $dA_g = e^{2s}\,dA_h$. Multiplying these yields $K_g\,dA_g = (K_h - \Delta_h s)\,dA_h$. Integrating over M, the Laplacian term $\int_M \Delta_h s\,dA_h$ vanishes identically by the divergence theorem. The seam's exact contribution perfectly cancels out globally, leaving $\int K_g\,dA_g = \int K_h\,dA_h = 2\pi\chi(M)$. □

Theorem 2 (Local non-degeneracy of the Hessian rule)**.** *Let M be a smooth manifold equipped with a torsion-free connection ∇. Let $s \in C^\infty(M)$ and define the symmetric $(0,2)$-tensor $g := \nabla^2 s$ (the covariant Hessian). If $p \in M$ is a point where g_p is positive definite, then g defines a Riemannian metric on some neighborhood of p.*

Proof. Positive definiteness is an open condition: since $q \mapsto g_q$ varies smoothly, there exists a neighborhood $U \ni p$ such that g_q remains positive definite for all $q \in U$. On U, g is therefore a smooth Riemannian metric. □

An open universality question. Beyond curvature identities, it is natural to ask whether composed scalar rules can approximate *arbitrary* Riemannian metrics in a suitable topology. We record this explicitly as an open problem in the conclusion (Open Problem 6).

5 Discrete Geometry and Computation

The true advantage of the seam framework is algorithmic. In this climax section, we prove that discrete graph rules strictly approximate continuous geometries, preserve curvature, and enable uniquely solvable inverse-design problems.

5.1 Quantitative Discrete-to-Continuum Limits

Lemma 1 (Vertex-path approximation of geodesics)**.** *Let (M, g_0) be compact and let $\{G_n = (V_n, E_n)\}$ be a sequence of weighted graphs with vertex sets $V_n \subset M$ and background edge lengths ℓ_0 induced by g_0. Assume V_n is an h_n-net in (M, d_{g_0}) with $h_n \to 0$, and assume the edges are uniformly local in the sense that $\ell_0(u, v) = O(h_n)$ for all $(u, v) \in E_n$. Fix points $x, y \in M$ and choose vertices $u_n, v_n \in V_n$ with $d_{g_0}(u_n, x) \le h_n$ and $d_{g_0}(v_n, y) \le h_n$. Assume in addition that the 1-skeleton is an* asymptotically geodesic spanner *for (M, g_0) in the sense that there exists a constant C_{span} (independent of n) such that for all sufficiently large n and all vertices $a, b \in V_n$ there exists a vertex path P from a to b with*

$$L_0(P) \le (1 + C_{\text{span}}\, h_n)\, d_{g_0}(a, b).$$

Then there exists a vertex path P_n in G_n from u_n to v_n such that its background length satisfies

$$L_0(P_n) \le d_{g_0}(x, y) + Ch_n,$$

where C depends only on (M, g_0) and the constants implicit in the assumptions above.

Proof. By the triangle inequality,

$$d_{g_0}(u_n, v_n) \le d_{g_0}(u_n, x) + d_{g_0}(x, y) + d_{g_0}(y, v_n) \le d_{g_0}(x, y) + 2h_n.$$

By the spanner assumption applied to $(a, b) = (u_n, v_n)$, there exists a vertex path P_n from u_n to v_n such that

$$L_0(P_n) \le (1 + C_{\text{span}}\, h_n)\, d_{g_0}(u_n, v_n) \le (1 + C_{\text{span}}\, h_n)\, (d_{g_0}(x, y) + 2h_n).$$

Since M is compact, $d_{g_0}(x, y) \le \operatorname{diam}(M, g_0)$, so the right-hand side is bounded by $d_{g_0}(x, y) + Ch_n$ for a constant C independent of n. □

Remark 5 (On the spanner assumption). The spanner hypothesis in Lemma 1 is the precise technical condition needed to convert continuous g_0-geodesic distances into comparable *edge-path* distances on the graph with an $O(h_n)$ error. Sampling/coverage alone ensures V_n is dense in M, but without a spanner-type assumption one may only obtain a mesh-dependent *multiplicative* distortion between graph shortest-path length and d_{g_0}. It is important to distinguish two related but different notions. (i) In the planar Euclidean setting, the Delaunay triangulation is a *geometric t-spanner* (for an explicit universal constant $t > 1$); see, e.g., [18]. This is a constant-factor guarantee. (ii) The hypothesis used

in Lemma 1 is stronger: it asks for an *asymptotically geodesic* spanner with stretch $1 + O(h_n)$, which is the ingredient that yields an *additive* $O(h_n)$ distance error for fixed $x, y \in M$. A constant-factor spanner bound alone does *not* imply such an asymptotically tight estimate.

For smooth manifolds, $(1 + o(1))$-type geodesic-graph approximation results are typically proved for sufficiently dense *neighborhood graphs* (e.g., ε-graphs or kNN graphs with neighborhood size tending to zero but containing many sample points), rather than for bounded-degree triangulation 1-skeleta; see, e.g., [19] for a representative uniform convergence statement in the Isomap setting. In our experiments we use Delaunay triangulations (for moderate n) and switch to symmetric kNN graphs for scalability; empirically the resulting shortest-path distances exhibit the expected $O(h)$ behavior in Figure 2.

For background on Delaunay triangulations and mesh generation (independent of spanner/stretch guarantees), see [20, 21].

Lemma 2 (Trapezoidal consistency of the conformal edge rule)**.** *Let $s \in C^2(M)$ and let $\gamma : [0, L] \to M$ be a unit-speed (g_0) geodesic segment. For a subsegment of length $\ell \le h$ with endpoints $p = \gamma(t_0)$ and $q = \gamma(t_0 + \ell)$, define the trapezoidal approximation*

$$T(p, q) := \ell \, \frac{e^{s(p)} + e^{s(q)}}{2}.$$

Then the conformal length satisfies

$$\left| \int_{t_0}^{t_0+\ell} e^{s(\gamma(t))} \, \mathrm{d}t - T(p, q) \right| \le C_s \, \ell^3,$$

where C_s depends on $\sup_M |\nabla^2(e^s)|$ (equivalently on $\sup_M(|\nabla s|, |\nabla^2 s|)$).

Proof. Since γ is unit-speed in the background metric g_0, the parameter t is exactly g_0-arc length along γ, i.e. $\mathrm{d}t = \mathrm{d}\ell_0$ on the segment. The claim is then the standard trapezoidal error estimate for C^2 functions: if $f(t) := e^{s(\gamma(t))}$, then $f \in C^2$ and the error on an interval of length ℓ is bounded by $\frac{\ell^3}{12} \sup |f''|$. Boundedness of f'' follows from $s \in C^2$ and compactness of M. □

Theorem 3 (Discrete-to-continuum limit via correspondences)**.** *Let (M, g_0) be a compact Riemannian manifold and $s \in C^2(M)$. Let $\{G_n = (V_n, E_n)\}$ be a sequence of weighted graphs with $V_n \subset M$ and mesh size $h_n \to 0$ such that the assumptions of Lemma 1 hold (in particular, V_n is an h_n-net and $\ell_0(u, v) = O(h_n)$ on edges). Let the discrete conformal graph metric d_n be generated by $\mathcal{R}_{\text{Graph-Exp } s}$ evaluated on V_n. Assume the asymptotically geodesic spanner property stated in Lemma 1 holds for G_n with respect to d_{g_0}. Then the Gromov–Hausdorff distance between (V_n, d_n) and (M, d_g) satisfies $d_{GH}\big((V_n, d_n), (M, d_g)\big) = O(h_n)$ (see, e.g., [7]), where $g := e^{2s} g_0$ and d_g is the induced geodesic distance on M.*

Proof. Define a correspondence $\mathcal{C}_n \subset V_n \times M$ by pairing each vertex $u \in V_n$ with itself viewed as a point in M, i.e. $\mathcal{C}_n := \{(u, u) : u \in V_n\}$. Since V_n is an h_n-net in M (by assumption), every $x \in M$ lies within g_0-distance $\le h_n$ of some $u \in V_n$, hence within g-distance $\le e^{\|s\|_\infty} h_n$ of some vertex as well. Thus $\mathcal{C}_n$ is an $O(h_n)$-surjective correspondence.

To bound the distortion, fix $u, v \in V_n$. By Lemma 1 (with $x = u$ and $y = v$), there exists a vertex path in the 1-skeleton from u to v with background length

$$L_0(P_n) \le d_{g_0}(u, v) + O(h_n).$$

Applying Lemma 2 edgewise along this path shows that the discrete conformal length of the path differs from the g-length of the corresponding piecewise-g_0-geodesic curve by at most $O(h_n^2)$, hence $d_n(u,v) \le d_g(u,v) + O(h_n)$. In particular, the dominant $O(h_n)$ term in this estimate comes from the spanner property in Lemma 1; the trapezoidal quadrature contributes only a higher-order $O(h_n^2)$ correction along a path.

For the reverse inequality, let $\widehat{P}_n = (p_0 = u, \dots, p_m = v)$ be a *discrete shortest path* attaining $d_n(u,v) = \sum_{i=0}^{m-1} w(p_i, p_{i+1})$. Form a continuous curve $\widehat{\Gamma}_n$ by concatenating the g_0-geodesic segments joining each (p_i, p_{i+1}). Then

$$d_g(u,v) \le L_g(\widehat{\Gamma}_n) = \sum_{i=0}^{m-1} \int_{p_i}^{p_{i+1}} e^s \, \mathrm{d}\ell_0.$$

Lemma 2 applied to each edge segment (with $\ell_0(p_i, p_{i+1}) = O(h_n)$) gives

$$\int_{p_i}^{p_{i+1}} e^s \, \mathrm{d}\ell_0 \le \ell_0(p_i, p_{i+1}) \, \frac{e^{s(p_i)} + e^{s(p_{i+1})}}{2} + O(h_n^3) = w(p_i, p_{i+1}) + O(h_n^3).$$

Summing over i and using $m = O(1/h_n)$ yields $L_g(\widehat{\Gamma}_n) \le d_n(u,v) + O(h_n)$, hence $d_g(u,v) \le d_n(u,v) + O(h_n)$. Therefore

$$\sup_{u,v \in V_n} \left| d_n(u,v) - d_g(u,v) \right| \le C h_n.$$

It follows that the distortion of $\mathcal{C}_n$ is $O(h_n)$, hence $d_{GH}\big((V_n, d_n), (M, d_g)\big) \le \frac{1}{2} \operatorname{dis}(\mathcal{C}_n) = O(h_n)$. □

While limits are mathematically satisfying, algorithms require quantitative bounds.

Theorem 4 (Quantitative metric error bound)**.** *Under the assumptions of Theorem 3, assume in addition that:*

1. *for the pairs of points under consideration, minimizing g-geodesics are unique and stay a fixed distance away from the cut locus (so the minimizing curves vary continuously with endpoints), and*
2. *G_n satisfies the asymptotically geodesic spanner property from Lemma 1 (so that edge paths approximate d_{g_0} up to an $O(h_n)$ relative error).*

Then there exists a constant $C > 0$ (depending on bounds of s, ∇s, $\operatorname{Hess} s$, and the mesh regularity) such that the discrete metric satisfies an $O(h_n)$ error bound relative to the continuous metric:

$$\sup_{u,v \in V_n} |d_n(u,v) - d_{e^{2s} g_0}(u,v)| \le C h_n \tag{5.1}$$

Remark 6 (On the cut locus assumption). The uniqueness/away-from-cut-locus hypothesis is strong: it rules out endpoint pairs for which multiple minimizing g-geodesics compete or where the minimizing curve changes discontinuously under small perturbations. It is included here to justify a *uniform* $O(h_n)$ bound stated as a supremum over vertex pairs; relaxing it typically requires either restricting to pairs avoiding the cut locus, working with local/one-sided estimates, or accepting weaker (e.g., measure-theoretic) error statements.

Proof. Fix vertices $u, v \in V_n$ and let $x = u$, $y = v$ be viewed as points of M. Let γ be a minimizing g-geodesic from x to y (under the additional hypotheses stated in the theorem). By Lemma 1 (applied to g_0) there exists a vertex path $P_n = (p_0 = u, \dots, p_m = v)$ whose background length satisfies $L_0(P_n) \le d_{g_0}(x, y) + Ch_n$.

Write $w_n(p_i, p_{i+1}) = \ell_0(p_i, p_{i+1}) \frac{e^{s(p_i)} + e^{s(p_{i+1})}}{2}$. Summing Lemma 2 edgewise along the polyline yields that the discrete conformal length of P_n differs from the corresponding conformal line integral by $O(h_n^2)$ (since each edge contributes $O(h_n^3)$ and there are $O(1/h_n)$ edges).

Thus, as in Theorem 3, the leading $O(h_n)$ contribution to the final distance error bound comes from the spanner approximation of g_0-geodesics by edge paths, while the trapezoidal consistency of the conformal edge rule contributes only a higher-order $O(h_n^2)$ term.

Taking the infimum over vertex paths gives $d_n(u, v) \le d_g(x, y) + C_1 h_n$; conversely, comparing any discrete shortest path to the continuous geodesic and using the same two lemmas yields $d_g(x, y) \le d_n(u, v) + C_2 h_n$. Combining the inequalities gives the stated uniform $O(h_n)$ bound. □

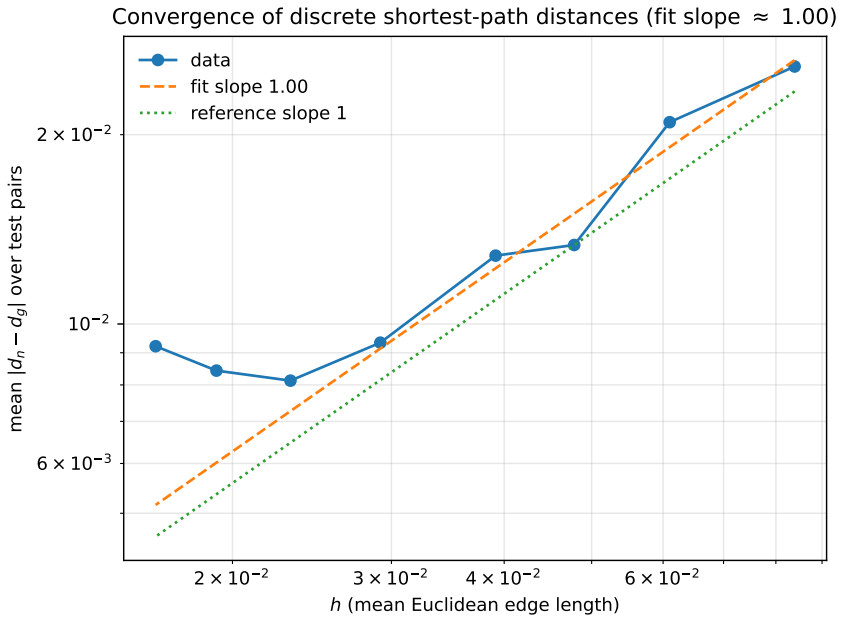

Figure 2: Log–log convergence plot for the discrete shortest-path metric: mean $|d_n - d_g|$ over fixed test pairs versus h (mean edge length) on a quasi-uniform sampling sequence with neighborhood-style graphs. A fit over the pre-plateau regime yields slope close to 1 (dashed), consistent with the $O(h)$ rate driven by the spanner approximation; the dotted line shows a slope-1 reference.

5.2 Algorithmic Stability and Inverse Design

We emphasize a basic but important distinction in what follows: the inverse-design problem we solve is posed at the level of *local geometry* (edge weights / discrete line elements). The resulting

global metric space structure is then induced as the shortest-path distance on the weighted graph. In particular, we do not fit all-pairs distances directly.

Theorem 5. *Let $G = (V, E)$ be a triangulated mesh (or any connected, non-bipartite graph) with background lengths $\ell_0(e) > 0$. Given an arbitrary, potentially noisy or invalid set of target edge weights $w^*(e) > 0$, the optimal seam s^* minimizing the squared error under the Conformal Graph Rule:*

$$\mathcal{E}(s) = \sum_{\{u,v\}\in E} \left(\ell_0(u,v) \frac{e^{s(u)} + e^{s(v)}}{2} - w^*(u,v) \right)^2 \tag{5.2}$$

can be found by solving a strictly convex quadratic program in the variables $X_u := e^{s(u)} > 0$.

Remark 7 (Local targets vs. induced metric). The targets $w^*(e)$ are edge-wise measurements and need not satisfy any global consistency constraints such as the triangle inequality. Once an optimizer X^* (hence seam s^*) is found, it defines seam-generated edge weights $w_{s^*}(e)$, and these weights induce a bona fide shortest-path metric D_{s^*} on V by construction. Thus the QP performs a projection at the level of local edge geometry, with the global metric obtained as the induced path metric.

Proof. Under the substitution $X_u = e^{s(u)}$, the energy $\mathcal{E}(X)$ becomes a quadratic function $\frac{1}{2}X^T HX - C^T X + K$. The Hessian H of this polynomial has diagonal entries $\sum_{v\sim u} \ell_0^2(u,v)/4$ and off-diagonal entries $\ell_0^2(u,v)/4$. This matrix H is exactly proportional to the *signless Laplacian* $Q = D + A$ of the weighted graph.

The spectral characterization we use here is classical: for a connected graph, the signless Laplacian Q is positive definite (equivalently, its smallest eigenvalue is > 0) if and only if the graph is non-bipartite (contains an odd cycle) [9, 10]; see also [8] for general spectral-graph background. Our contribution is not this spectral fact, but the observation that the conformal graph rule makes inverse edge-weight fitting reduce *exactly* to such a quadratic form in $X = e^s$, yielding a practically solvable strictly convex program on non-bipartite graphs. Because a triangulation contains 3-cycles, it is non-bipartite and thus $H \succ 0$ in that case. Therefore, $\mathcal{E}(X)$ is strictly convex, guaranteeing a unique global minimum $s^* = \ln X^*$. □

Remark 8 (Positivity constraint). Strict convexity holds for the quadratic objective in X, but the change of variables imposes $X_u > 0$. Thus the natural optimization problem is a strictly convex QP with simple positivity constraints (or an unconstrained problem if one works directly in s, where the objective is generally *not* quadratic). If the unconstrained quadratic minimizer $X^* = H^{-1}b$ fails to satisfy $X^* > 0$ (which can occur for severely distorted targets w^*), then the appropriate object is the constrained optimizer of the convex QP with bounds $X \geq 0$ (or $X \geq \varepsilon$ for a small floor), obtained from the KKT system or an active-set/NNLS-type solve. Geometrically, an active bound $X_u \downarrow 0$ corresponds to driving $s(u) = \log X_u \to -\infty$, i.e., forcing the conformal factor at u to collapse. Under our *arithmetic-mean* edge rule, this does not automatically send all incident edge lengths to zero (since $\ell_s(u,v) = \ell_0(u,v)\frac{1}{2}(X_u + X_v) \to \ell_0(u,v)\frac{1}{2}X_v$ when $X_u \to 0$), but it does make the vertex u contribute negligibly to the local scaling and indicates a degenerate/singular limit of the seam-generated metric around u.

Theorem 6 (Gauge fixing and conditioning for inverse design)**.** *Under the assumptions of Theorem 5, write the quadratic objective in X as*

$$\mathcal{E}(X) = \tfrac{1}{2} X^\top H X - b^\top X + K,$$

with $H \succ 0$ (for non-bipartite connected graphs). Then:

1. ***Uniqueness (gauge-fixed).*** *The minimizer X^* is unique. Moreover, if one imposes a normalization constraint (a "gauge") such as $\sum_{u \in V} X_u = 1$, the constrained minimizer is also unique.*
2. ***Conditioning and stability.*** *For the unconstrained minimizer $X^* = H^{-1} b$, perturbations satisfy the Lipschitz bound*

$$\|\delta X^*\|_2 \le \|H^{-1}\|_2 \, \|\delta b\|_2 = \frac{1}{\lambda_{\min}(H)} \, \|\delta b\|_2.$$

In particular, the inverse design problem is well-conditioned when $\lambda_{\min}(H)$ is bounded away from 0.

Proof. Since $H \succ 0$, the unconstrained quadratic $\mathcal{E}$ is strictly convex and has a unique minimizer characterized by the first-order condition $\nabla \mathcal{E}(X) = HX - b = 0$, hence $X^* = H^{-1} b$.

For the gauge-fixed problem with affine constraint $a^\top X = 1$ (e.g. $a = \mathbf{1}$), strict convexity of $\mathcal{E}$ implies uniqueness of the constrained minimizer as well (the restriction of a strictly convex function to an affine subspace is strictly convex). Existence holds since the feasible set is nonempty and closed.

For stability, differentiate the optimality condition: $(H + \delta H)(X^* + \delta X^*) = (b + \delta b)$. Keeping only first-order terms in perturbations yields $H \, \delta X^* = \delta b - (\delta H) X^*$. In the common setting where only b varies (targets w^* change while H is fixed by the background mesh), this reduces to $H \, \delta X^* = \delta b$ and thus $\delta X^* = H^{-1} \delta b$. Taking 2-norms gives the claimed bound with $\|H^{-1}\|_2 = 1/\lambda_{\min}(H)$. □

Remark 9 (Interiority vs. positivity constraints). Theorem 6 is stated for the unconstrained quadratic minimizer. The same conditioning estimate applies to the positivity-constrained QP in Theorem 5 whenever the optimizer lies in the interior of the feasible set (i.e., $X_u^* > 0$ for all u), since then the KKT system reduces to $HX = b$. If active positivity constraints occur, the solution map is still Lipschitz on regions of constant active set, with an analogous bound involving the reduced Hessian. From a modeling perspective, persistent active constraints (many vertices with X_u pinned at the boundary) are a diagnostic that the targets w^* are far from the realizable set of seam-generated edge weights, or that additional regularization/prior information on s is needed to avoid metric degeneracy.

5.3 Curvature Preservation

Finally, we prove that our specific arithmetic graph rule perfectly captures continuous geometric curvature logic.

Theorem 7. *Let $G = (V, E)$ be a triangulated surface with background lengths ℓ_0. Let $K_s(u) = 2\pi - \sum \theta_t$ be the discrete Gaussian curvature (angle defect) induced by the seam-generated edge lengths $\ell_s(u, v) = \ell_0(u, v) \frac{e^{s(u)} + e^{s(v)}}{2}$. The Jacobian of the curvature with respect to the seam, evaluated at $s = 0$, is exactly:*

$$\left. \frac{\partial K_s(u)}{\partial s(v)} \right|_{s=0} = L_{uv}^{cot} \tag{5.3}$$

where L^{cot}_{uv} is the cotangent Laplacian matrix with off-diagonal convention

$$L^{cot}_{uv} := -\tfrac{1}{2}\big(\cot\alpha_{uv} + \cot\beta_{uv}\big) \quad (u \neq v),$$

in which α_{uv} and β_{uv} denote the angles opposite *the edge (u, v) in the two incident triangles (and $L^{cot}_{uu} := -\sum_{v\neq u} L^{cot}_{uv}$).*

Proof. Fix an arbitrary perturbation $\dot{s} : V \to \mathbb{R}$ and consider the 1-parameter family $s(t) := t\dot{s}$ with induced edge lengths

$$\ell_t(u, v) = \ell_0(u, v)\,\frac{e^{s(t)(u)} + e^{s(t)(v)}}{2}.$$

Differentiating at $t = 0$ gives the first variation

$$\dot{\ell}(u, v) := \left.\frac{\mathrm{d}}{\mathrm{d}t}\right|_{t=0} \ell_t(u, v) = \ell_0(u, v)\,\frac{\dot{s}(u) + \dot{s}(v)}{2}. \tag{5.4}$$

Now compare this to the *classical* discrete conformal scaling on triangle meshes, in which one uses

$$\widetilde{\ell}_t(u, v) := \ell_0(u, v)\exp\Big(\tfrac{1}{2}\big(s(t)(u) + s(t)(v)\big)\Big).$$

At $t = 0$, the first variation of $\widetilde{\ell}_t$ agrees with (5.4) as well:

$$\left.\frac{\mathrm{d}}{\mathrm{d}t}\right|_{t=0} \widetilde{\ell}_t(u, v) = \ell_0(u, v)\,\frac{\dot{s}(u) + \dot{s}(v)}{2}.$$

Since triangle angles (hence angle defects) are smooth functions of the edge lengths in a nondegenerate Euclidean triangle, it follows by the chain rule that the first variation of the curvature map $s \mapsto K_s$ at $s = 0$ is the same for our arithmetic-mean rule and for the classical exponential-length rule.

For the classical rule, the first variation of angle-defect curvature is standard (see, e.g., [15, 13, 11]): for an interior edge (u, v) with opposite angles α_{uv}, β_{uv} in the two incident triangles,

$$\dot{K}(u) = \sum_{v\sim u} \tfrac{1}{2}\big(\cot\alpha_{uv} + \cot\beta_{uv}\big)\,\big(\dot{s}(u) - \dot{s}(v)\big),$$

with the natural modification at boundary edges (only one incident triangle). Equivalently, in matrix form $\dot{K} = L^{\cot}\,\dot{s}$, where $L^{\cot}$ has off-diagonal entries $L^{\cot}_{uv} = -\frac{1}{2}(\cot\alpha_{uv} + \cot\beta_{uv})$ for $u \neq v$ and diagonal entries $L^{\cot}_{uu} = -\sum_{v\neq u} L^{\cot}_{uv}$.

Because this holds for every perturbation $\dot{s}$, it identifies the Jacobian of K_s with respect to s at $s = 0$, proving the claim. □

Remark 10 (Linearization at $s = 0$: feature vs. limitation). Theorem 7 is intentionally stated at $s = 0$: it identifies the *exact first-order* response of discrete curvature to an infinitesimal seam perturbation around the background metric ℓ_0. This should be read as a *feature* when the goal is differentiable geometry processing: it provides a closed-form Jacobian (a sparse cotangent Laplacian) that can be used directly as a gradient/Hessian building block or as a preconditioner inside seam-optimization loops.

It is also a genuine *limitation* if one expects a globally valid curvature-control law: for finite seams, the map $s \mapsto K_s$ is nonlinear (through both the exponential edge rule and the triangle-angle dependence on lengths), so the Jacobian generally varies with s. In practice one can either (i) re-linearize at the current iterate by recomputing the corresponding cotangent-type operator on the seam-generated geometry, or (ii) differentiate K_s numerically/automatically through the angle formulas. Our use of Theorem 7 is therefore as a principled first-order curvature sensitivity tool, not as a claim that curvature control remains linear far from $s = 0$.

5.4 Numerical Validation

To complement the theoretical results, we validate the inverse-design quadratic program (Theorem 5) on random geometric graphs. The reference implementation is publicly available at `https://github.com/Roenbaeck/seams`.

We generate graphs with $n \in \{10^2, 10^3, 10^4\}$ vertices and assign a ground-truth seam s_{gt}. Ground-truth edge weights w_{gt} are generated via the conformal graph rule. We then form noisy target weights $w^*(u,v) = w_{\text{gt}}(u,v)(1 + \sigma\xi_{uv})$, where ξ_{uv} is i.i.d. standard normal noise and $\sigma \in [0, 0.20]$ controls the noise level. For $n \leq 5000$ we use a Delaunay triangulation; for larger n we use a symmetric k-nearest-neighbor graph for scalability. We solve the strictly convex QP to recover the optimal seam s^* and its induced weights w_{opt}.

In practice, our Python/NumPy/SciPy implementation solves the unconstrained normal equations for the quadratic objective via a sparse direct solve (with a small ridge for numerical stability), with a nonnegativity-constrained least-squares fallback when needed (SciPy's `nnls` for small n and `lsq_linear` with bounds for large n). On a typical laptop, the core inverse-design solve (excluding shortest-path evaluation) takes about 0.04 seconds for $n = 10^4$.

Table 2 summarizes the results. The optimization consistently denoises the metric: for instance, at $n = 10^4$ and $\sigma = 0.10$, the noisy weights deviate from the truth by 9.9%, while the recovered weights w_{opt} reduce this error to 5.3%. This denoising effect extends to the induced shortest-path metric, where the mean relative path error drops from 5.0% (noisy) to 2.3% (recovered). The reported R^2 values are consistently high across the sweep, supporting the proof-of-concept that the seam parameterization can explain a large fraction of the variance in the target edge weights even under noise. The lone low-R^2 outlier ($n = 100, \sigma = 0.20$) reflects an expected failure mode: at very small n with heavy noise, the target weights are insufficiently informative and the seam-generated model cannot explain the majority of the variance. Furthermore, finite-difference checks confirm that the analytical derivatives and Hessian-vector products match numerical finite differences to high precision (worst relative errors $\sim 10^{-6}$ and $\sim 10^{-9}$ over the sweep), validating the exactness of the quadratic formulation.

Finally, we empirically visualize the predicted $O(h)$ convergence of the discrete shortest-path metric to the continuous conformal metric (Theorems 3–4) by comparing discrete distances on quasi-uniform sampling sequences with neighborhood-style graphs against a high-resolution grid-based approximation of the continuous geodesic distance. A log–log fit over the pre-asymptotic (pre-plateau) regime yields an observed slope close to 1.

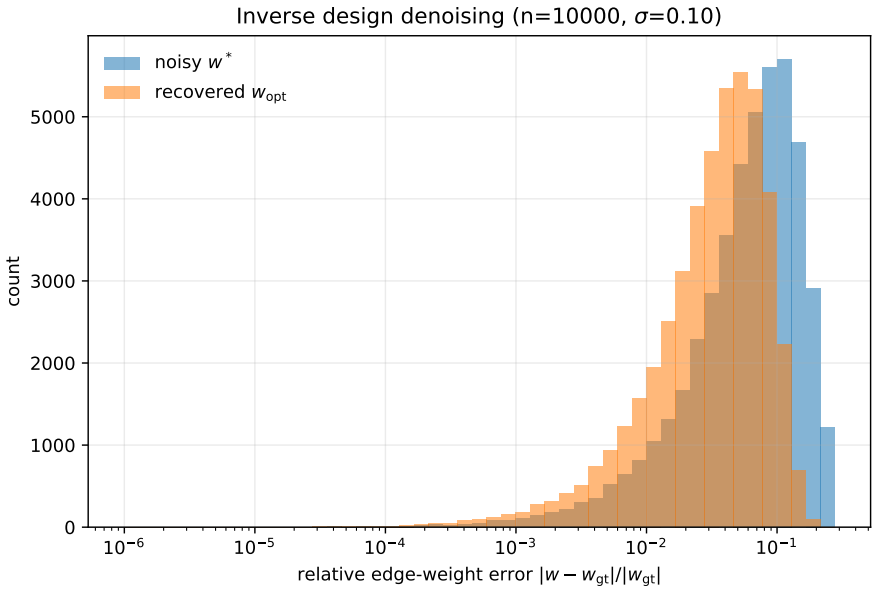

Figure 3: Inverse-design denoising: histogram of relative edge-weight error with respect to ground truth, comparing noisy targets w^* to recovered weights w_{opt} obtained from the strictly convex inverse-design solve.

6 Conclusion and Open Problems

Seam-Driven Geometry reframes continuous and discrete metric spaces as the structured output of scalar functions. In geometry processing terms, the seam is not merely a parameterization: it is a stable interface between continuous differential-geometric objectives and discrete optimization primitives.

The theorems established here open immediate applications in machine learning and geometry processing:

- **Metric Nearness Projection:** Theorem 5 shows that "repairing" noisy, physically invalid edge weights on a graph reduces to a strictly convex quadratic program in a scalar field (in variables $X = e^s$), solvable with standard sparse linear-algebra machinery rather than $O(N^3)$ semidefinite programming.
- **Intrinsic Metric Editing and Conformal Design:** The conformal graph rule provides a lightweight intrinsic metric design primitive for meshes, supporting tasks such as curvature-aware metric editing and conformal-style rescalings that integrate naturally with discrete conformal pipelines [13, 12].
- **Isotropic Sizing Fields for Remeshing/LOD (Outlook):** Interpreting the seam as a scalar sizing field suggests a simple route to isotropic remeshing and level-of-detail control by locally expanding or contracting intrinsic lengths, without introducing full anisotropic metric tensors.

Table 2: Numerical validation of inverse seam design. The optimization recovers edge weights (w_{opt}) that are significantly closer to the ground truth (w_{gt}) than the noisy targets (w^*), and similarly improves shortest-path distances. The inverse-design step is solved via sparse linear algebra (normal equations with a positivity-constrained least-squares fallback); for $n = 10^4$ the core solve takes about 0.04 s in our reference implementation (excluding shortest-path evaluation).

n	$\lvert E\rvert$	σ	Weight Error (to w_{gt})		Path Error (Mean Rel.)		R^2
			Noisy w^*	Recov. w_{opt}	Noisy	Recov.	
100	286	0.05	0.053	0.034	0.018	0.019	0.979
100	286	0.10	0.107	0.068	0.034	0.035	0.914
100	286	0.20	0.213	0.136	0.073	0.071	0.122
1,000	2,978	0.05	0.050	0.040	0.012	0.011	0.986
1,000	2,978	0.10	0.100	0.080	0.027	0.024	0.943
1,000	2,978	0.20	0.201	0.160	0.075	0.065	0.766
10,000	46,229	0.05	0.050	0.026	0.017	0.008	0.994
10,000	46,229	0.10	0.099	0.053	0.050	0.023	0.974
10,000	46,229	0.20	0.198	0.105	0.144	0.067	0.900

- **Shape comparison via scalar representatives (Outlook):** In settings where shapes can be mapped (or registered) to a common background domain and represented primarily by a conformal factor, the geometry is captured by a scalar seam. This suggests practical surrogates for comparing and interpolating geometries by operating directly on seam fields (with curvature sensitivity guided by Theorem 7), rather than manipulating dense all-pairs distances.
- **Graph Neural Network (GNN) Rewiring:** A major bottleneck in GNNs is "oversquashing," where information chokes at structural bottlenecks. Standard rewiring destroys topology. Our Conformal Graph Rule allows a neural network to learn a seam s that dynamically "stretches" bottlenecks (altering edge weights to increase local flow) while rigorously preserving the original topological adjacency and spectral validity of the graph.
- **Seam-based metric learning for embeddings (Outlook):** Many visualization and embedding pipelines search for point positions in a fixed ambient space. An alternative suggested by the seam viewpoint is to keep a simple background domain fixed (e.g., a grid or mesh) and instead learn the intrinsic metric on that domain by optimizing a seam s, so that geodesic distances in the learned metric better match observed dissimilarities.

Open Problem (Universality). Let M be a compact smooth manifold and fix a background metric h. Consider the family of symmetric $(0,2)$-tensors obtained from scalar seams $s \in C^\infty(M)$ by applying any finite composition of admissible scalar-to-tensor Rules from the seam repertoire (e.g., conformal and Hessian-type constructions), and then forming finite positive linear combinations whenever the result is positive definite.

Is this family dense in the space of smooth Riemannian metrics on M in the uniform (C^0) topology on tensor fields? If not, what is the weakest natural extension of the repertoire (additional rule types, allowing diffeomorphism reparameterizations, etc.) that yields a genuine

density/universality statement?

Future Work. Future work will focus on extending the discrete optimal transport ($\mathcal{R}_{\mathrm{OT}}$) rules to dynamic multi-agent pathfinding, and exploring whether sums of composed seam rules can act as universal approximators for smooth metrics.

Remark 11 (Differentiable seam learning and GNN rewiring). For learning-based pipelines, a seam s_θ produced by a neural network can be optimized end-to-end by differentiating through a *relaxed* shortest-path layer (e.g., via log-sum-exp/softmin path energies or entropic optimal transport relaxations). The seam parameterization provides a low-dimensional, geometry-aware control knob: backpropagated gradients update s while preserving the underlying adjacency, and Theorem 6 gives a linear-algebraic handle on conditioning when the edge-fitting objective is used as a loss.

Acknowledgments

The author gratefully acknowledges assistance from large language models (Gemini 3.1, GPT-5.2, Grok 4.2, Sonnet 4.6) for drafting, proof polishing, and numerical scripting, under the author's full conceptual and mathematical oversight.

References

[1] S.-I. Amari, *Information Geometry and Its Applications*, Springer Japan, Tokyo, 2016.

[2] H. Shima, *The Geometry of Hessian Structures*, World Scientific, 2007.

[3] P. Petersen, *Riemannian Geometry*, 2nd ed., Springer, 2006.

[4] J. A. Sethian, *Level Set Methods and Fast Marching Methods*, 2nd ed., Cambridge University Press, 1999.

[5] J. Milnor, *Morse Theory*, Princeton University Press, 1963.

[6] R. M. Wald, *General Relativity*, University of Chicago Press, 1984.

[7] D. Burago, Y. Burago, and S. Ivanov, *A Course in Metric Geometry*, American Mathematical Society, 2001.

[8] F. R. K. Chung, *Spectral Graph Theory*, American Mathematical Society, 1997.

[9] M. Desai and V. Rao, "A characterization of the smallest eigenvalue of a graph," *Journal of Graph Theory* **18**(2), 181–194 (1994).

[10] D. Cvetković, P. Rowlinson, and S. K. Simić, "Signless Laplacians of finite graphs," *Linear Algebra and its Applications* **423**, 155–171 (2007).

[11] A. I. Bobenko and B. A. Springborn, "A discrete Laplace–Beltrami operator for simplicial surfaces," *Discrete & Computational Geometry* **38**, 740–756 (2007).

[12] X. Gu, F. Luo, J. Sun, and T. Wu, "A discrete uniformization theorem for polyhedral surfaces," *Journal of Differential Geometry* **109**, 223–256 (2018).

[13] B. Springborn, P. Schröder, and U. Pinkall, "Conformal equivalence of triangle meshes," *ACM Transactions on Graphics* **27**(3) (2008).

[14] K. Crane, U. Pinkall, and P. Schröder, "Spin transformations of discrete surfaces," *ACM Transactions on Graphics* **32**(4) (2013).

[15] U. Pinkall and K. Polthier, "Computing discrete minimal surfaces and their conjugates," *Experimental Mathematics* **2**(1), 15–36 (1993).

[16] B. Chow and F. Luo, "Combinatorial Ricci flows on surfaces," *Journal of Differential Geometry* **63**, 97–129 (2003).

[17] K. Stephenson, *Introduction to Circle Packing: The Theory of Discrete Analytic Functions*, Cambridge University Press, 2005.

[18] J. Mark Keil and C. A. Gutwin, "Classes of graphs which approximate the complete Euclidean graph," *Discrete & Computational Geometry* **7**, 13–28 (1992).

[19] J. B. Tenenbaum, V. de Silva, and J. C. Langford, "A global geometric framework for nonlinear dimensionality reduction," *Science* **290**(5500), 2319–2323 (2000).

[20] J. R. Shewchuk, "Delaunay refinement algorithms for triangular mesh generation," *Computational Geometry* **22**(1–3), 21–74 (2002).

[21] F. Aurenhammer, R. Klein, and D.-T. Lee, *Voronoi Diagrams and Delaunay Triangulations*, World Scientific, 2013.